Journal of the European Ceramic Society 22 (2002) 1297–1306

www.elsevier.com/locate/jeurceramsoc

Rheological properties of tin oxide suspensions

Iêda Maria Garcia dos Santos[d,*], Antônio Gouveia de Souza[b], Fabrício Ronil Sensato[a], Edson Roberto Leite[a], Elson Longo[a], José Arana Varela[c]

[a]*LIEC, Departamento de Química, UFSCar, Rod. Washington Luis, km 235, CP 676, cep 13565-905, São Carlos, SP, Brazil*
[b]*LTM, Departamento de Química/CCEN/UFPB, Cidade Universitária, Campus I, cep 58059-900, João Pessoa, PB, Brazil*
[c]*Universidade Estadual Paulista, Instituto de Química, r. Prof. Francicsco Degni, s/n, cep 14800-900, Araraquara, SP, Brazil*
[d]*Universidade Federal da Paraiba, Departamento de Química, Cidade Universitária, Campus 1, cep 58059-900 João Pessoa, PB, Brazil*

Received 11 January 2001; received in revised form 2 August 2001; accepted 15 August 2001

Abstract

The rheological properties of tin oxide slurries were studied experimentally and theoretically. The deflocculants used were ammonium polyacrilate (PAA) and the copolymer poly(vinyl butyral-*co*-vinyl alcohol-*co*-vinyl acetate) (PVB-PVA-PVAc), in water and ethanol, respectively. The amount of deflocculant was optimized for different solid contents by means of viscosity measurements. In spite of the high stability of PVB-dispersed slurries, a high solid concentration was not obtained. On the other hand, a slurry with a 56.4 vol.% of solids was attained when PAA was used. A theoretical study of the adsorption of PAA in its dissociated (basic solution) and non-dissociated (acidic solution) forms on SnO_2 (110) is presented. This analysis was made by means of the PM3 method using a large cluster $Sn_{15}O_{28}$ for the surface model. The calculated adsorption energy is larger for the ionized PAA than for the non-ionized form, indicating that alkaline slurries favor PAA adsorption on the SnO_2 surface.

Keywords: Adsorption; Deflocculants; Modelling-adsorption; Rheology; SnO_2

1. Introduction

Tin oxide has been used in contact with glasses containing lead, being commonly used as electrode material.[1,2] Shaw[1] emphasizes the advantages of the use of this refractory material in the melting of lead silicate, leading to a reduction in the volatilization of lead oxide and reduced pollution. It also produces a final product with improved quality, since tin oxide does not tint glass.

The use of tin oxide crucibles made by slip casting to process corrosive materials has proved to be promising for technological applications. Tin oxide crucibles have been employed successfully to melt glasses containing heavy metal oxides[3] and fluorides[4], and to process $Y_1Ba_2Cu_3O$ single crystals.[5] The properties of glasses melted in tin oxide crucibles are similar to those melted in platinum or gold crucibles, indicating the possible substitution of these crucibles by tin oxide ones that are less costly.

A study of the rheological properties of tin oxide slurries is required to produce high quality crucibles. Little research has been done in this area due to the difficulties involved in obtaining high density materials after sintering. Astanina et al[6] have produced stable slurries containing 60–85% of solids (mass percent) using sodium carboxymetilcelulose and sodium silicate as deflocculants, used both separately and together. Pron'kina et al.[7] tested different deflocculants and concluded that carboxymetilcelulose is an efficient one.

The viscosity of the slurry, considering particles as rigid spheres, is directly related to the volumetric fraction of solids. In high concentrations, the interactions between the particles affect rheological behavior. Many models have been proposed in an attempt to include the hydrodynamic and Brownian interactions, but agreement with the experimental results has only been qualitative. On the other hand, semi-empirical models, such as the Krieger–Dougherty [Eq. (1)] and the Quemada [Eq. (2)] are commonly used.[8]

* Corresponding author. Tel.: +55-83-216-7441; fax: +55-83-216-7441.

E-mail address: ieda@labpesq.quimica.ufpb.br (I.M. Garcia dos Santos).

0955-2219/02/$ - see front matter
PII: S0955-2219(01)00440-X

$$\eta_r = \left(1 - \frac{\phi}{\phi_m}\right)^{-[\eta]\phi_m}, \quad (1)$$

$$\eta_r = \left(1 - \frac{\phi}{\phi_m}\right)^{-2}, \quad (2)$$

where ϕ_m is the maximum attainable volumetric fraction, ϕ is the volumetric fraction, (η) is the intrinsic viscosity (2.5 for spheres) and η_r is the relation between the viscosity of the suspension and that of the solvent.

Besides the adsorbed polymer, sterically stabilized slurries also involve a slight repulsion between particles. In practice, these factors lead to an increase in the attainable volume of particles and consequently, in the volumetric fraction of the solid phase. In this case, the effective volume fraction may be calculated using, for example, the Barker and Henderson equation.

$$a_{eff} = a + 1/2\int_{2\alpha}^{\infty}\{1 - \exp[U(R)/k_B T]\}dR, \quad (3)$$

$$\phi_{eff} = \phi\left(\frac{a_{eff}}{a}\right)^3, \quad (4)$$

where a is the particle diameter and $U(R)$ is the pair interaction potential.[8]

The present work consisted of a study of the rheological properties of tin oxide slurries dispersed with polyacrylic acid (PAA) and polyvinylbutyral. To obtain high density crucibles, 0.5% mol of manganese oxide was added to the tin oxide, according to Cerri et al.,[9] who obtained ceramic pellets with a density above 99%.

In relation to the theoretical calculations, the aim of this work was to use semiempirical techniques to investigate the electronic structure of a SnO_2 system in order to understand the rheological properties of SnO_2 at the molecular level and to rationalize the role played by the oxygen vacancies in the interaction between SnO_2 particle surface and PAA.

Several theoretical studies using different models have investigated both the electronic properties and interaction between several adsorbates and SnO_2.[10] Quantum chemical calculations were made to further analyse the influence of both pH and SnO_2 particles on polymer configuration.

2. Materials and methods

2.1. Experimental procedure

The rheological properties of tin oxide (99.9%—CESBRA) suspensions, doped with 0.5 mol% of manganese oxide (Aldrich Chemical Co.), were determined by means of viscosity measurements (Brookfield—DV III), with variation of the deflocculant type and concentration, solvent, solid concentration and pH.

Powder characterization before milling was done by means of BET (Micromeritics, ASAP 2000) analysis and particle size distribution (Horiba, CAPA 500). The surface area was 5.40 m^2/g, with a mean particle size estimated from this surface area of 0.16 μm. In relation to particle size distribution, the material presents a mean particle size of 0.3 μm. These particle sizes cannot be compared because particle size analyzers typically favor particles that are micron size and larger, while surface area analyzers tend to favor the fine particle fractions.[11]

The polymers poly(vinylbutyral-*co*-vinylalcohol-*co*-vinylacetate)–PVB/PVA/PVAc (Aldrich Chemical Co.) and ammonium polyacrylate (IQAPAC C, IQA) were used as deflocculants. Absolute ethanol (Mallinkrodt) was used as the solvent in the first system and distilled water in the second. The amount of solids varied from 12.6 to 56.4 vol.%. All the suspensions were milled in an attritor mill for 30 min at a speed of 500 rpm. Alumina balls with 2 mm of diameter were used as grinding media.

The optimized amount of deflocculant was determined through the addition of progressive amounts of deflocculant, followed by viscosity measurements at different shear rates. After optimization of the deflocculant quantity, a sedimentation test was carried out. The pH optimization was done through the addition of pure ammonium hydroxide (Merck), with the use of a 10 μl micropipette, followed by a viscosity measurement.

2.2. Theoretical procedure

SnO_2 crystallizes in the rutile structure, which has a tetragonal D_4^{14} symmetry. There are two formula units per primitive unit cell, with the three-fold coordinated oxygen atoms forming a distorted octahedron around the tin atoms. An experimental analysis shows that the (110) surface is the most stable SnO_2 face.[12] However, the SnO_2 (110) surface can be obtained at different oxidation degrees, depending on the experimental conditions: stoichiometric, reduced, and defective.[13] The material readily loses surface oxygen because of the variable valence of Sn, giving rise to a reduced surface. In this case, electrical neutrality is maintained when the Sn^{4+} ions on the surface ionic plane are reduced to Sn^{2+}, according to Eq. (5):

$$SnO \xrightarrow{SnO2} Sn''_{Sn} + V^{\bullet\bullet}_{O} + O^{x}_{O}, \quad (5)$$

In this context, a large $Sn_{15}O_{30}$ cluster model (see Fig. 1a for Moviemol[14] diagram), derived from crystallographic data[15] was selected to represent the ideal SnO_2 (110) surface. The reduced SnO_2 (110) surface model was made by removing two bridging oxygens in positions 44

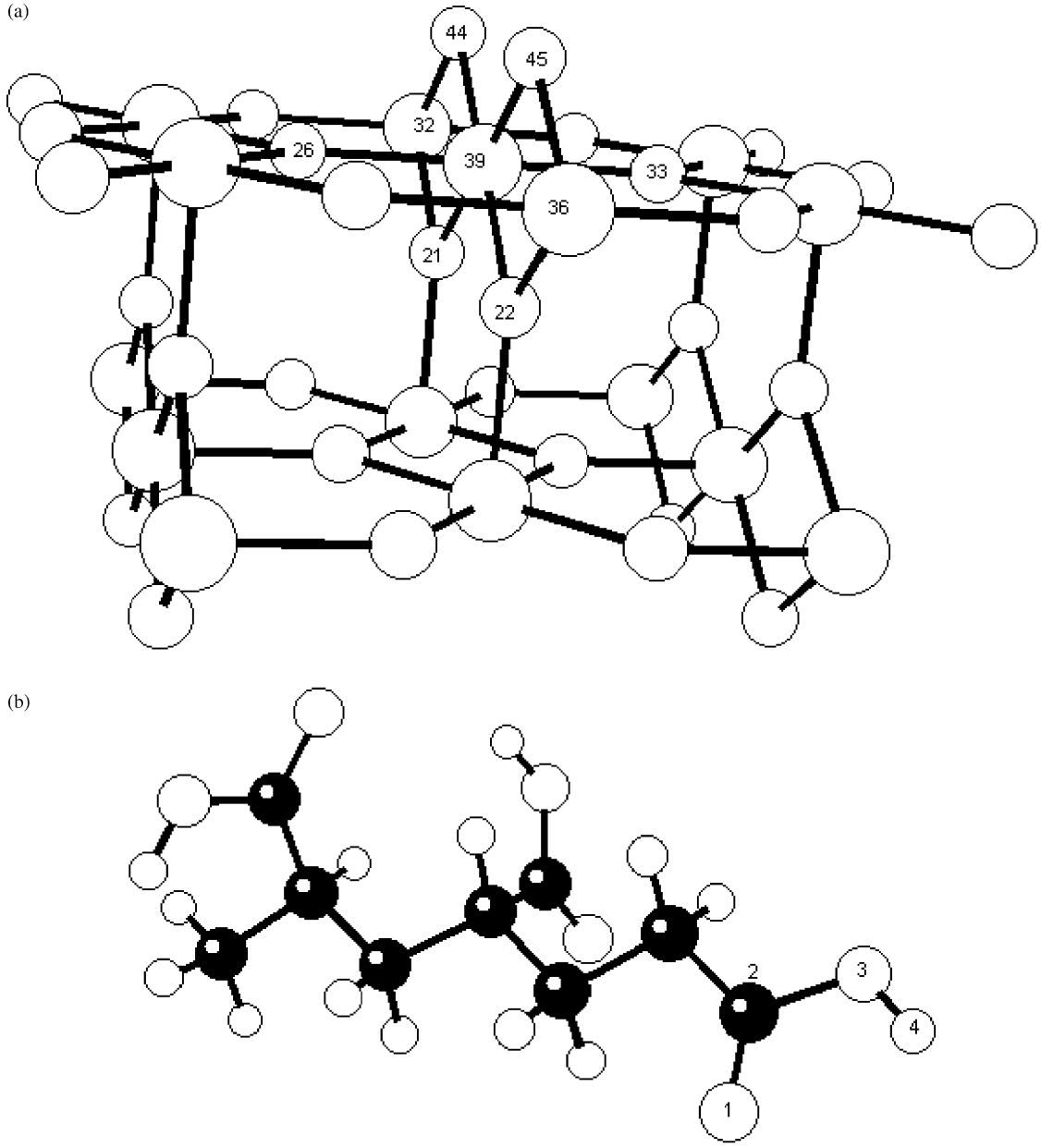

Fig. 1. Structural drawing of: (a) Nonrelaxed structure of a basic $Sn_{15}O_{30}$ cluster representing the ideal SnO_2 (110) surface. The large and small balls are, respectively, tin and oxygen atoms. (b) Theoretical equilibrium geometry for PAA. Large and small open circles represent O and H atoms, respectively; the dark circles represent C atoms.

and 45, according to Eq. (5), leading to the $(SnO_2)_{13}$ $(SnO)_2$ cluster model, which meets the requirements of stoichiometry and neutrality and has, therefore, been chosen to be used throughout this report.

The cluster approach was chosen because it is particularly well suited to tackle local phenomena such as single adsorbates on a surface.[16] Generally, surface relaxation effects are important in chemisorption, which is why, in this study, relaxation of the (110) surface of SnO_2 was considered. Once the relaxation of the reduced SnO_2 (110) surface was reached, the $(SnO_2)_{13}(SnO)_2$ cluster geometry was frozen during all the calculations, whereas the absorbed PAA and PAA^- geometries (Fig. 1b) were fully optimized. PAA^- was obtained from the PAA structure by removing a hydrogen atom H(4), followed by full optimization of the geometry.

To understand the characteristic of PAA adsorption on the reduced SnO_2 (110) surface as a function of pH, the interactions of tin oxide with PAA in its non-dissociated (acidic solution) and dissociated forms (basic solution) were investigated. For a quantum chemical study of such a system size, semiempirical methods were employed extensively. Although the specificity of these methods could be called into question, they are

computationally and physically applicable. Therefore, calculations were made with the PM3[17] semiempirical methods included in the GAUSSIAN 94 program package.[18]

The interaction energy between the cluster and the PAA with three monomeric units was calculated according to Eq. (6):

$$E_{ads} = Et_{(Sn_{15}O_{28}+PAA)} - Et_{Sn_{15}O_{28}} - Et_{PAA}, \quad (6)$$

where $Et_{(Sn_{15}O_{28}+PAA)}$ is the energy of the adsorbate/substrate system, $Et_{Sn15O28}$ is the energy of the substrate and Et_{PAA} is the total energy of the isolated adsorbate and its theoretical equilibrium geometry.

3. Results and discussion

3.1. Viscosity measurements

PVB copolymer efficiency in ethanol was tested in different solid concentrations (12.6–25.1 vol.%). The deflocculant used had an average molecular weight (M_n) of 42,584 daltons and a maximum molecular weight (M_w) of 118,886 daltons, with a polydispersivity (M_w/M_n) of 2.79.

It is well known that PVB copolymer acts as a steric stabilizer and that its efficiency depends on the solvent's quality.[19] What part of the copolymer is adsorbed on the particle's surface is still a controversial issue. While it is usually assumed that adsorption is due to PVB, Parker and Sacks studied copolymers containing different amounts of PVA and demonstrated that adsorption on the alumina increases as the amount of PVA increases.[20]

The behavior of the suspension was determined through plots of log σ versus log γ, according to Eq. (7):[19]

$$\sigma = k\ \gamma^m \quad (7)$$

where k is a constant related to viscosity, σ is the shear stress and γ is the stress rate. The m value indicates flux behavior, thus:

- $m < 1$ indicates pseudoplasty,
- $m = 1$ indicates Newtonian behavior and
- $m > 1$ indicates dilatancy.

The m values are plotted in Fig. 2. All the curves presented a high coefficient of linear regression ($r > 0.99$). Only the suspension having a 21.1 vol.% of solids and a 3.8 wt.% of deflocculant showed almost Newtonian behavior. All the suspensions were pseudoplastic when the PVB concentration was low, indicating flocculation. As the concentration increased, the rheological behavior became dilatant, which is characteristic of highly loaded suspensions with a high repulsive force between particles.[19] The suspension having a 25.1 vol.% of solids presented pseudoplastic behavior, indicating poor dispersion. In other words, PVB is not efficient in dispersing concentrated suspensions (>21 vol.%).

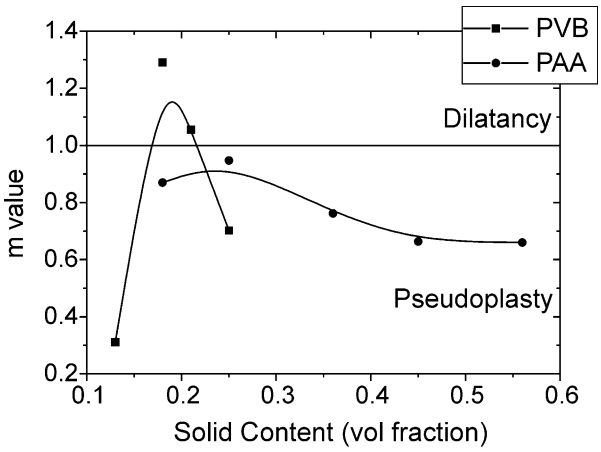

Fig. 2. Graph illustrating the behavior of the slurries, according to the m-values as a function of the solid content, using optimized amount of deflocculant.

The behavior of viscosity as a function of deflocculant concentrations was also investigated, as shown in Fig. 3. Except for the suspension with a 25.1 vol.% of solids, the viscosities of the other suspensions did not increase with increasing PVB content after reaching the minimum value of viscosity. The optimized amount of deflocculant is presented in Table 1.

In relation to the low solid concentration attained, one possible reason for the inefficient dispersion was the choice of solvent. This may be due to the low solubility of PVB in ethanol. In this case, the probability of polymer adsorption on the particle surface increases due to the low interaction polymer-liquid, which leads to a dense covering and, consequently, prevents the particles from approaching each other. On the other hand, a good solvent results in an increase in deflocculant efficiency owing to the formation of loops and tails extending from the surface of the particle into the liquid.[19]

A similar study was also carried out for PAA. The deflocculant used had an average molecular weight (M_n) of 9308 daltons, a maximum molecular weight (M_w) of 63,027 daltons and a polydispersivity (M_w/M_n) of 6.77.

Table 1
Optimized amount of defloculant for the different suspensions

Solid content	Media	Deflocculant	% Deflocculant
17.7	Ethanol	PVB	1.52
21.1	Ethanol	PVB	3.80
17.7	Water	PAA	0.30
25.1	Water	PAA	0.20
36.5	Water	PAA	0.15
44.9	Water	PAA	0.16
56.4	Water	PAA	0.16

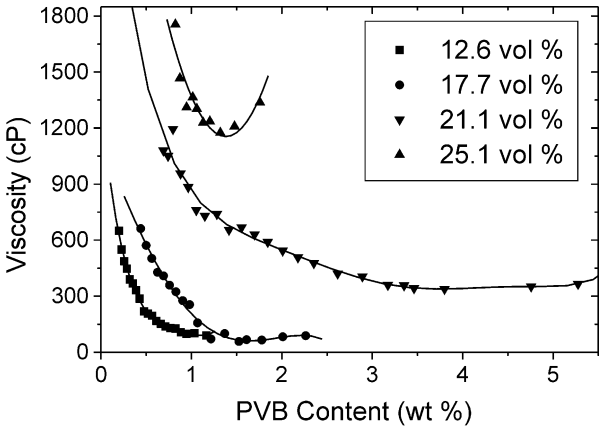

Fig. 3. Viscosity curves as a function of the PVB concentration in different solid contents.

In this case, distilled water was used as solvent and the concentration of solids varied from 17.7 to 56.4 vol.%.

Ammonium polyacrilate is a polyelectrolite and its dispersion mechanism is electrosteric. The structure of polyacrilate is:

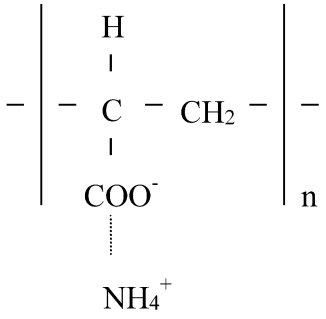

and it dissociates in water, according to Eqs. (8) and (9):[21]

$$PAA - NH_4 \Longleftrightarrow PAA^- + NH_4^+ \quad (8)$$

$$PAA^- + H_2O \Longleftrightarrow PAA - H + OH^- \quad (9)$$

The log σ versus log γ curves were obtained and the m values were calculated and plotted in Fig. 2. As before, all the curves presented a high coefficient of linear regression ($r > 0.99$).

Only the suspension with a 25.1 vol.% of solids presented a nearly Newtonian behavior, the others presenting pseudoplastic behavior. Additionally, it can be observed that the pseudoplasty increased as the solid concentration increased. This fact is probably related to higher particle interaction. The structure of a colloidal suspension in rest is the result of a balance between the interparticle potential and the Brownian particle motion.[8] When the solid concentration is very high, the repulsive force between particles is insufficient to prevent their interaction, and agglomerates are formed with water inside them. As the shear rate increases, agglomerates are broken and the water inside them is released leading to a decrease in viscosity. The suspension with a 17.7 vol.% of solids is pseudoplastic due to the low efficiency of PAA in the dispersion of low concentrated suspensions. This fact can also be observed in the deflocculant optimization curves shown in Fig. 4. This figure shows the decrease in the optimized amount of deflocculant as the solid concentration increases, up to a limit of 56.4 vol.% of solids, which presents an increase in the optimized amount of PAA.

Another important point is the increased viscosity of the suspensions with solid concentrations above 36.5% after the addition of higher amounts of deflocculant. According to Hirata, this may be due to electrostatic repulsion between: (i) free charged polymers and (ii) negatively charged free polymers and free polymers adsorbed in the particle.[22]

The optimized amount of deflocculant is presented in Table 1.

3.2. Sedimentation measurements

Figs. 5 and 6 illustrate the sedimentation study. The results obtained show that suspensions dispersed with PVB are highly stable, particularly the suspension with a 21.1 vol.% of solids (Fig. 6a). This stability indicates that the polymer is efficiently adsorbed on the tin oxide and on the manganese oxide, preventing the separation between the suspension's constituents.

Fig. 5 indicates the formation of a black region, consisting of manganese oxide, above a gray region, consisting of tin oxide, in suspensions dispersed with PAA. This is due to the separation between manganese oxide and tin oxide after 24 h. This effect is less pronounced in the less concentrated suspensions. Apparently, PAA adsorption on manganese oxide is more efficient than on tin oxide, leading to a higher concentration of MnO_2 at the top of the essay tube and a higher concentration of

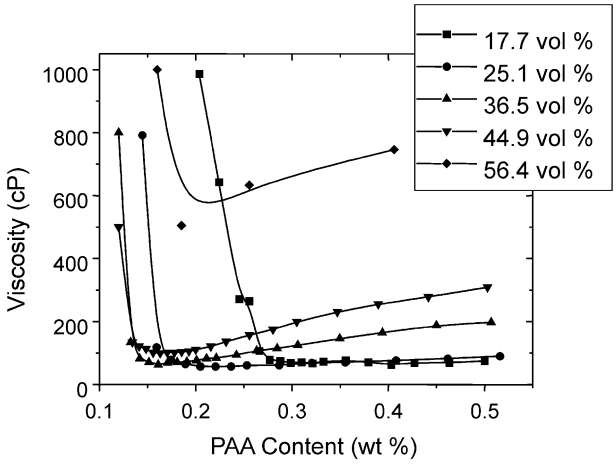

Fig. 4. Viscosity curves as a function of the PAA concentration in different solid contents.

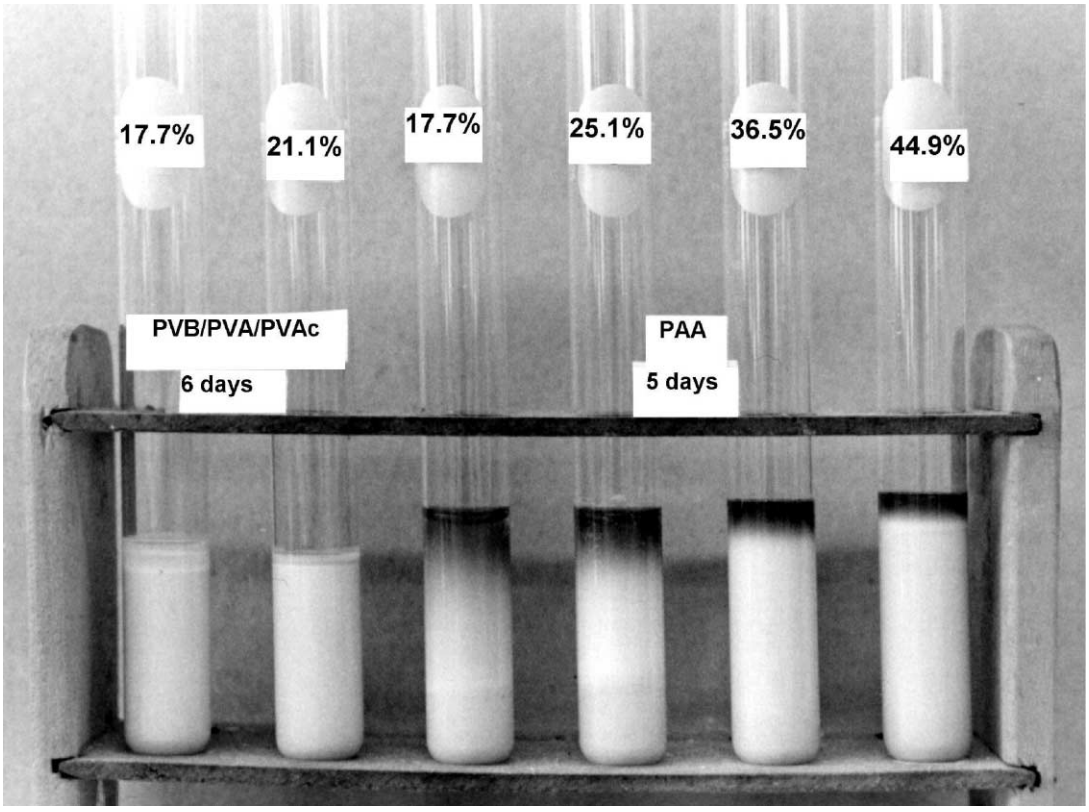

Fig. 5. Photograph showing the result of the sedimentation test of the suspensions, using optimized amount of deflocculant.

SnO_2 at the bottom. After some time, the MnO_2 in the less stable suspensions also sediments, as shown in Fig. 7. It was also observed that the height of the liquid region is smaller in more concentrated suspensions.

3.3. pH test

pH tests were performed for PAA stabilized suspensions containing 44.9 and 56.4 vol.% of solids, as shown in Fig. 8. One can observe that viscosity decreases as pH increases. In higher pH values ($pH > 10$), the addition of a large amount of NH_4OH (10% of the total amount of water) is needed to change the pH, and the decreased viscosity may result from a higher dilution of the suspension.

Many authors have ascribed the influence of pH variation in polymer configuration to the surface charge of particles and of the polymer and, thus, to the amount of polymer adsorbed.

According to Biggs and Healy,[23] at pH values above the pzc (point of zero charge), the negative sites of ammonium polyacrylate repel each other, leading to an extended conformation. In addition, an electrostatic repulsion between polymer and surface occurs, because both are negatively charged and adsorption occurs in the few positive sites on surface. These effects lead to formation of loops and tails in the adsorbed configuration. As pH decreases, the polyelectrolyte chains become neutral and a highly collapsed conformation is acquired. As a consequence, more adsorbed chains are needed to cover particle surface. Moreover, a lower amount of charge in a solution decreases the magnitude of electrostatic repulsion between particles. Dispersion is, therefore, favored by higher pH values. The schematic diagram is presented in the Fig. 9.

A change in suspension behavior (from pseudoplastic to dilatant) with increasing pH was also observed. As mentioned earlier, dilatancy is characteristic of highly charged suspensions, where the repulsive force between particles is high.[19]

3.4. Quantum chemical studies

Several calculations in which PAA and PAA^- molecules were positioned at different starting configurations were made. These calculations take into account favorable electrostatic interaction between the adsorbate molecule and the relaxed surface.

Results obtained are shown in Fig. 10 and indicate that PAA^- molecules (in ionized form) adsorb in a perpendicular mode[23] on SnO_2 and their adsorption energy has been estimated at -89.2 kcal mol^{-1}. A C(2)-O(1)-Sn(39)-O(21)-Sn(32)-O(3) six-membered structure is formed (numbers in brackets indicate the number of the atoms in the Fig. 10). The value of the O(1)–C(2)–O(3) bond angle decreases to around 10° and the distances

between the two oxygens of the terminal carboxyl [O(1) and O(3)] and the Sn(39) and Sn(32) become 2.085 and 2.117 Å, respectively. Thus, the O(3) occupies roughly the same position with respect to the tin as would be taken by oxygen in the bulk crystal [see O(44) at Fig. 1a].

Electron distribution was computed according to Mulikeńs partition scheme.[24] A charge transfer of 0.42 e^- from PAA^- towards to (110) SnO_2 surface was observed. An analysis of each atom indicated that the strongest charge is distributed between the oxygen atoms bonded to the Sn(32) and Sn(39) in the plane of interaction O(26), O(29), O(33) and O(34). The pertinent net charges are as follows: Sn(32) = 1.46; Sn(36) = 1.31; Sn(39) = 1.96;

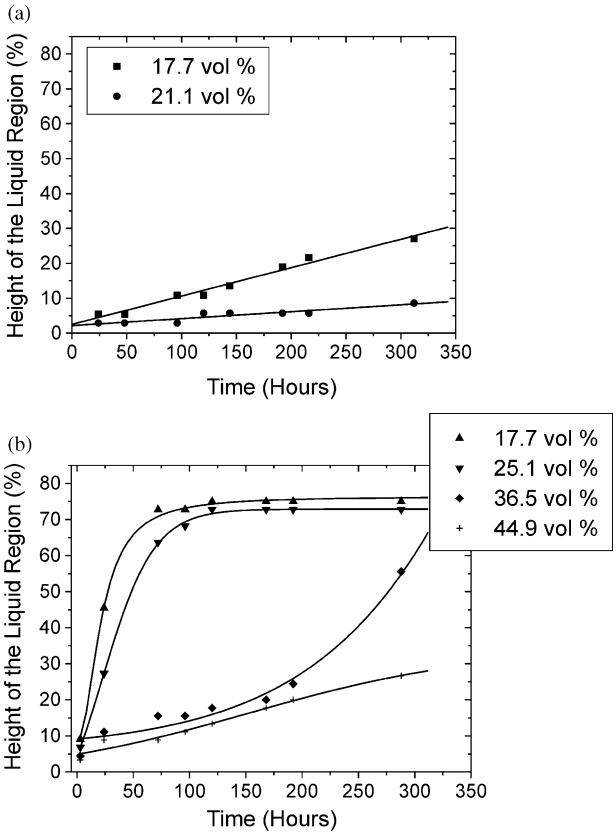

Fig. 6. Sedimentation test of the suspensions, using optimized amount of deflocculant. (a) Slurries dispersed with PVB; (b) Slurries dispersed with PAA. Height of the liquid region (in percentage) was measured as the height of the liquid region divided by the total height of the material in the essay tube.

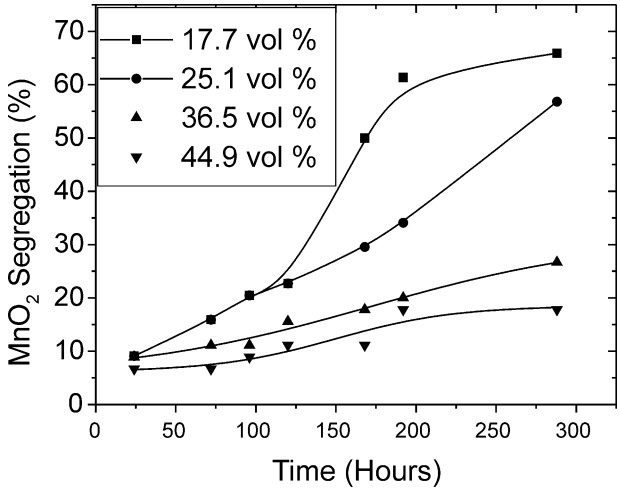

Fig. 7. MnO_2 segregation formed during the sedimentation test of the suspensions, using optimized amount of deflocculant. Segregation percentage was measured as the height of the black region divided by the total height of the material in the essay tube.

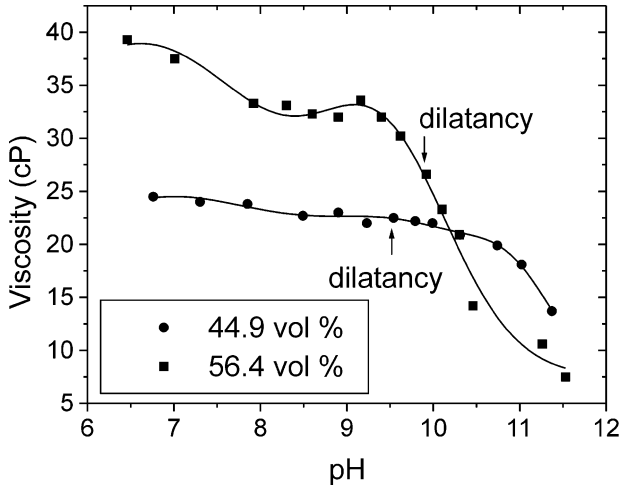

Fig. 8. Relation between viscosity and pH, for slurries dispersed with PAA in different solid contents, using optimized amount of deflocculant.

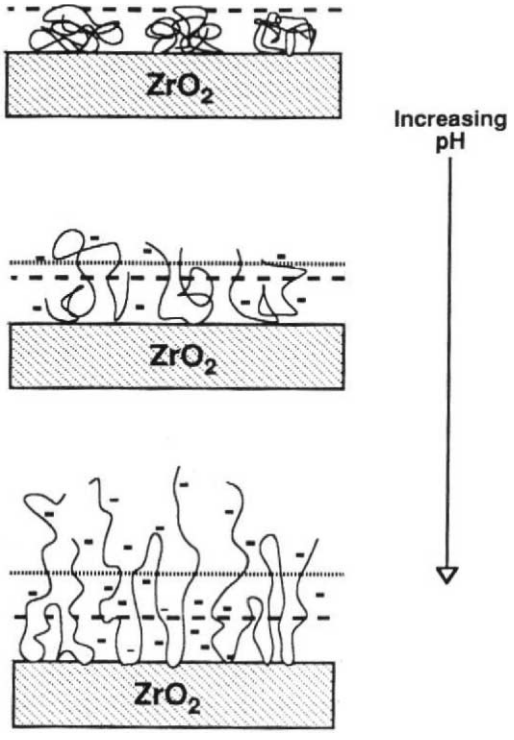

Fig. 9. Schematic diagram of the changing conformation of adsorbed PAA on ZrO_2 as a function of increasing pH.[23]

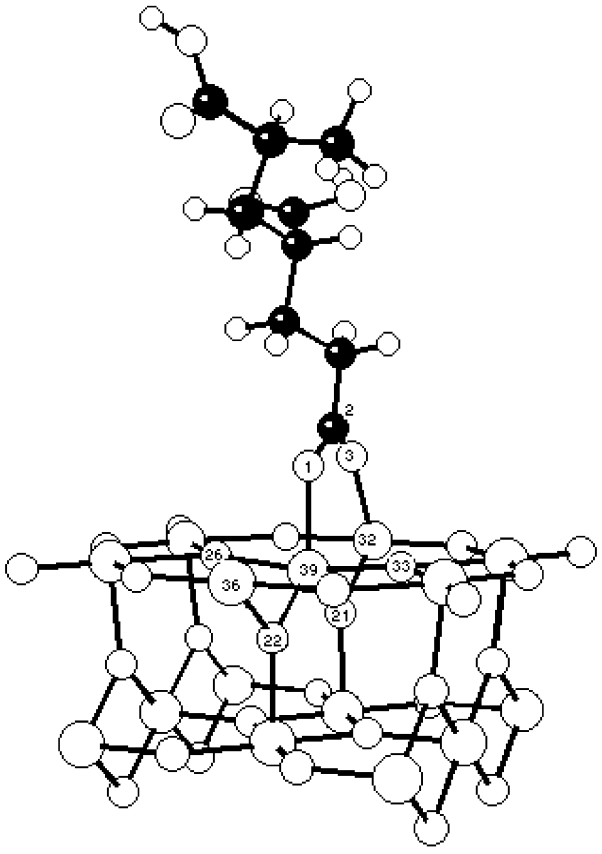

Fig. 10. Arrangement of the $(SnO_2)_{13}(SnO)_2$ cluster and PAA-(ionized) after optimization. The lighter large and small balls are, respectively, tin and oxygen. The darker balls represent carbon atoms while hydrogen atoms are represented by even smaller light balls.

O(26) = −1.01; O(33) = −1.01; O(1) = −0.59; O(3) = −0.62; and C(2) = 0.57.

PAA also takes on a perpendicular conformation on the reduced SnO_2 (110) surface but, contrary to PAA, the adsorption energy is slightly endothermic (5.5 kcal mol^{-1}). The distance between the oxygen of the terminal carboxyl [O(1)] and the Sn(39) becomes about 2.824.

These values are in agreement with the experimental results related to pH measurements. A higher pH favors PAA adsorption, increases the efficiency of steric stabilization and, thus, decreases viscosity. As soon as the pH decreases, the conditions for PAA adsorption are less favorable and viscosity increases.

3.5. Modeling for highly concentrated suspensions

Considering the present system as consisting of rigid spheres of the same size, Krieger–Dougherty [Eq. (1)] and Quemada [Eq. (2)] developed semi-empirical models to describe slurry behavior. Both models consider that the flux is affected only by viscous hydrodynamic interactions and by the Brownian motion. These models were used in this work to attempt to predict the behavior of tin oxide suspensions, dispersed with PAA, containing different solid concentrations.

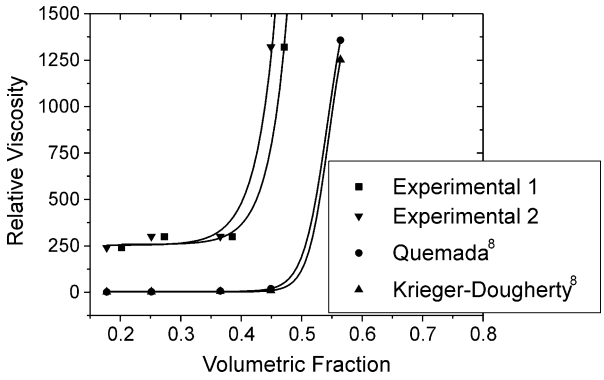

Fig. 11. Comparison between the applied models and the experimental data, for suspensions using optimized amount of deflocculant, considering the volumetric fraction [Eq. (1)] and the effective volumetric fraction [Eq. (2)].

Two plots were made based on the experimental results. The first plot considered the volumetric fraction of solids as being only the ceramic particles. The second plot considered the effective volumetric fraction, i.e. the ceramic particles with the adsorbed polymer. For this calculation, it was considered that the entire polymer in solution is adsorbed onto the particle in a plain conformation. The result obtained shows that agreement with the plots is only qualitative and the experimental curves are very similar, according to Fig. 11. It is important to note that the curves obtained from the two different models are also very similar.

The disagreement observed may be due to different factors, such as particle size distribution, which is not monomodal for the powder used. Thus, packing between particles increases as soon as smaller particles fill the empty space between bigger particles, leading to increased viscosity, particularly when the suspensions are more concentrated. Another possible reason is the non-uniformity of the liquid layer formed between the particles, which may change the viscous flux. A correction factor should be used when applying the Krieger–Dougherty and Quemada models to tin oxide suspensions dispersed in distilled water with PAA.

4. Conclusion

The results obtained show the possibility of obtaining stable suspensions with high solid concentrations (56.4 vol.%), using PAA as deflocculant. It was demonstrated that PVB is a good deflocculant giving suspensions which are very stable. The problem related to PVB is the low concentration of solids obtained. PAA presents higher stability for more concentrated suspensions. It was not possible to obtain a Newtonian behavior since the high solid concentration increases interparticle

interaction. The experimental and theoretical results indicate that an alkaline medium favors deflocculation, leading to stronger interaction between PAA and the reduced SnO_2 (110) surface.

Acknowledgements

This research was supported by grants from the Brazilian foundations: FAPESP, PRONEX/FINEP AND CNPq. We are also indebted to the Centro Nacional de Processamento de Alto Desempenho in São Paulo (CENAPAD-SP), and to the Centro Nacional de Supercomputação (CESUP-RS) for providing us with multiple computing facilities.

References

1. Shaw, G. B., Properties of tin oxide electrodes for the glass industry. *Glass Int*., 1987, **9**, 39–42.
2. Pavlovskii, V. K., Semenov, A. D. and Sobolev, Y. S., Corrosion of tin oxide materials in molten lead-silicate glass. *Steklo i Keramika*, 1990, **9**, 12–13.
3. Cerri, J. A., Santos, I. M. G., Longo, E., Leite, E. R., Lebullenger, R. M., Hernandes, A. C. and Varela, J. A., Characteristics of $PbO–BiO_{1.5}–GaO_{1.5}$ glasses melted in SnO_2 crucibles. *J. Am. Ceram. Soc*., 1998, **81**, 705–708.
4. Lebullenger R., *et al*. submitted to *J. Non-Crystal Sol*.
5. Rojas-Ramírez, R. A., *Crescimento de Monocristais Supercondutores $YBa_2Cu_3O_7$ — pelo método de fluxo em Cadinhos de SnO_2*. Mastering thesis, Universidade Federal de São Carlos, São Carlos, SP, Brazil, 1998.
6. Astanina, G. I., Kucheryavyi, M. N., Selyanko, V. T. and Balkevich, V. L., Properties of tin dioxide suspensions. *Glass Int*., 1982, **4**, 205–209.
7. Pron'kina, T. I., Zhuravina, T. A. and Mel'nikova, I. G., Slip casting of cassiterite ceramics. *Steklo i Keramika*, 1977, **2**, 26–27.
8. Pugh, R. J. and Bergström, L., *Surface and Colloid Chemistry in Advanced Ceramics Processing*. Marcel Decker, New York, 1994 pp. 204–208.
9. Cerri, J. A., Leite, E. R., Gouvea, D., Longo, E. and Varela, J. A., Effect of cobalt (II) and manganese (IV) oxide on sintering of tin (IV) oxide. *J. Am. Ceram. Soc*., 1996, **79**, 799–804.
10. (a) Munnix, S. and Schmeits, M., Electronic-structure of tin dioxide surfaces. *Phys. Rev. B*. 1983, **27**, 7624–7635; (b) Dobrovol'skii, Yu. A., Krupnov, B. V. and Zyubina, T. S., Simulation of carbon-dioxide chemisorption at the surface of an oxide electrode. *Russian J. Electrochem*. 1993, **29**, 1313–1318; (c) Godin, T. J. and LaFemina, J. P., Surface atomic and electronic-structure of cassiterite SnO_2 (110). *Phys. Rev. B*. 1993, **47**, 6518–6523; (d) Rantala, T. S., Lantto, V. and Rantala, T. T., A cluster approach for the SnO_2 (110) face. *Sensors and Actuators B*. 1994, 19, 716–719.; (e) Skafidas, P. D., D Vlachos, S. and Avaritsiotis, J. N., Modeling and simulation of tin oxide-based thick-film gas sensors using monte-carlo techniques. *Sensors and Actuators B*, 1994, **19**, 724–728; (f) Zyubina, T. S. and Dobrovol'skii, Yu. A. Cation transport over the oxide surface. *Russian J. Electrochem*. 1995, **31**, 1280–1284; (g) Manassidis, I., Goniakowski, J., Kantorovich, L. N. and Gillan, M. J., The structure of the stoichiometric and reduced sno2(110) surface. *Surf. Sci*. 1995, **339**, 258–271; (h) Martins, J. B. L., Longo, E., Andres, J. and Taft, C. A., Theoretical-study of cluster-models and molecular-hydrogen interaction with SnO_2 [110] surface. *J. Mol. Struct. (Theochem)*. 1995, **335**, 167–174; (i) Antunes, S. R. M., Santos, J. D., Antunes, A. C., Longo, E. and Varela, J. A., MNDO Theoretical-study of ethanol decomposition process on SnO_2 surfaces. *J. Mol. Struct. (Theochem)*. 1995, **357**, 153–159; (j) Camargo, A. C., Igualada, J. A., Beltrán, A., Llusar, R., Longo, E. and Andrés., An ab initio perturbed ion study of structural properties of TiO_2, SnO_2, and GeO_2 rutile lattices. *J. Chem. Phys*. 1996, **212**, 281–391; (k) Goniakowski, J. and Gillan, M. J., The adsorption of H_2O on TiO_2 and SnO_2 (110) studied by first-principles calculations. *Surf. Sci*. 996, **350**, 145–158; (l) Goniakowski, J., Holender, J. M., Kantorovich, L. N., Gillan, M. J. and White, J. A., Influence of gradient corrections on the bulk and surface properties of TiO_2 and SnO_2. *Phys. Rev. B: Condensed. Matter*. 1996, **53**, 957–960; (m) Sensato, F. R., Longo, E., Bulhões, L. O. S., Santos, J. D. and Martins, J. B. L., A theoretical study of lithium ion interaction with tin oxide. *J. Mol. Struct. (Theochem)*. 1997, **394**, 259–265; (n) Yamaguchi, Y., Nagasawa, Y., Murakami, A. and Tabata, K., Stability of oxygen anions and hydrogen abstraction from methane on reduced SnO_2 (110) surface. *Int. J. Quantum Chem*. 1998, 69, 669–678; (o) Rantala, T. T., Rantala, T. S. and Lantto, V., Surface relaxation of the (110) face of rutile SnO_2. *Surf. Sci*. 1999, **422**, 103–109; (p) Calatayud, M., Andrés, J. and Beltrán, A., A theoretical analysis of adsorption and dissociation of CH_3OH on the stoichiometric SnO_2 (110) surface. *Surf. Sci*. 1999, **430**, 213–222.
11. Dinger, D. R. and Funk, J. E., Particle-size analysis routines available on CERABULL: the PCI program. *Ceram. Bull*., 1990, **69**, 326–330.
12. Henrich, V. E. and Cox, P. A., *The Surface Science of Metal Oxides*, 1st edn. Cambridge University Press, Cambridge, 1994.
13. (a) Gercher, V. A., Cox, D. F. and Themlin, J., Oxygen-vacancy-controlled chemistry on metal-oxide surface-methanol dissociation and oxidation on SnO_2 (110). *Surf. Sci*. 1994, **306**, 279–293; (b) Gercher, V. A. and Cox, D. F., Formic-acid decomposition on SnO_2 (110). *Surf. Sci*. 1994, 312, 106–114; (c) Gercher, V. A. and Cox, D. F., Water-adsorption on stoichiometric and defective SnO_2 (110) surfaces. Surf. Sci. 1995, 322, 177–184.
14. Hermansson, K. and Ojamae, L., University of Uppsala, Institute of chemistry, Report UUIC-B19-500, 1994.
15. Baur, V. W., Uber die verfeinerung der kristallstrukturbestimmung einiger vertreter des rutiltyps—TiO_2, SnO_2, GeO_2 und MgF_2. *Acta Crystallogr*, 1956, **9**, 515–520.
16. Sauer, J., Molecular-models in ab initio studies of solids and surfaces—from ionic-crystals and semiconductors to catalysts. *Chem. Rev*., 1989, **89**, 199–255.
17. Stewart, J. J. P., Optimization of parameters for semiempirical methods. 1. method. *J. Comp. Chem*., 1989, **10**, 209–220.
18. Frisch, M. J., Trucks, G. W., Schlegel, H. B., Gill, P. M. W., Johnson, B. G., Robb, M. A., Cheeseman, J. R., Keith, T. A., Petersson, G. A., Montgomery, J. A., Raghavachari, K., Al-Lahan, M. A., Zakrzewski, V. G., Ortiz, J. V., Foresman, J. B., Cioslowski, J., Stefanov, B. B., Nanayakkara, A., Challacombe, M., Peng, C. Y., P Ayala,Y., Chen, W., Wong, M. W., Andres, J. L., Replogle, E. S., Gomperts, R., Martin, R. L., Fox, D. J., Binklet, J. S., Defrees, D. J., Baker, J., Stewart, J. P., Head-Gordon, M., González, C. and Pople, J. A., *GAUSSIAN 94*, Gaussian Inc., Pittsburgh, PA, 1995.
19. Bhattacharjee, S., Paria, M. K. and Maiti, H. S., Polyvinyl butyral as a dispersant for barium titanate in a non-aqueous suspension. *J. Mater. Sci*., 1993, **28**, 6490–6495.
20. Parker, A. A., Poly(vinylbutyral-co-vinyl alcohol) tacticity and aluminum-oxide surface-adsorption. *Macromolecules*, 1994, **27**, 7363–7368.
21. Wei, W. J., Lu, S. J. and Yu, B., Characterization of submicron alumina dispersions with poly(methacrylic acid) polyelectrolyte. *J. Eur. Ceram. Soc*., 1995, **15**, 155–164.

22. Hirata, Y., Nishimoto, A. and Ishihara, Y., Effects of addition of polyacrylic ammonium on colloidal processing of α-alumina. *J. Ceram. Soc. Jpn*., 1992, **100**, 983–990.
23. Biggs, S. and Healy, T. W., Eletrosteric stabilisation of colloidal zirconia with low molecular weight polyacrylic acid. *J. Chem. Soc. Faraday Trans*., 1994, **90**, 3415–3421.
24. Mulliken, R. S., Electronic population analysis on LCAO-MO molecular wave funcions. 1. *Chem. Phys*., 1955, **23**, 1833–1840.